Replacing measurement feedback with coherent feedback for quantum state preparation

Yoshiki Kashiwamura and Naoki Yamamoto

Department of Applied Physics and Physico-Informatics, Keio University, Hiyoshi 3-14-1, Kohoku, Yokohama 223-8522, Japan

Measurement feedback is a versatile and powerful tool, although its performance is limited by several practical imperfections resulting from classical components. This paper shows that, for some typical quantum feedback control problems for state preparation (stabilization of a qubit or a qutrit, spin squeezing, and Fock state generation), the classical feedback operation can be replaced by a fully quantum one such that the state autonomously dissipates into the target or a state close to the target. The main common feature of the proposed quantum operation, which is called coherent feedback, is that it is composed of a series of dispersive and dissipative couplings inspired by the corresponding measurement feedback scheme.

I. INTRODUCTION

Many quantum information systems contain *measurement feedback* (MF) processes such as teleportation and error correction [1]. However, the classical components involved in such processes introduce practical imperfections due to detection loss, time delays in the signal processing, and the finite bandwidth of actuators, which as a result severely limit the system performance. Thus, the following important question arises; can we replace those classical components by fully quantum systems that emulate the same functionalities?

The theory for MF is well established [2–6]. In particular, the MF control method based on quantum nondemolition (QND) measurement followed by filtering (i.e., continuous-time state estimation) has been investigated in depth [7–13] and some notable experiments have been demonstrated [14–19]. Figure 1 illustrates the idea of this MF control, for the case of squeezed state generation, as follows.

(1) The initial state is the vacuum.

(2) The system dispersively interacts with a probe field, and thereby they are entangled; if we measure the output field, the estimated system state becomes a squeezed state with random amplitude conditioned on the measurement result. The figure shows the ensemble of these conditional states.

(3) Finally, the measurement result is fed back to compensate this random displacement for generating the target squeezed state deterministically.

This paper gives an answer to the question posed above. That is, for some typical quantum feedback control problems for state preparation, we show that the classical operation that compensates the random displacement (i.e., the feedback process in Fig. 1) can be replaced by a fully quantum operation such that the state autonomously dissipates into the target or a state close to the target. Our idea is to use the *coherent feedback* (CF) scheme to realize this quantum operation; i.e., a quantum system is controlled via another quantum system in a feedback way that does not involve any measurement process. The CF scheme is implementable in a variety of systems including optics, superconductors, and cold atoms. See [20–28] for the basic theories and applications of CF,

and [29–34] for experimental demonstrations. Note that the control problem considered in this paper is not contained in the framework where the superiority of CF over MF (or the equivalency of CF and MF) has been proved [20,24–26,28,33]. Also the proposed scheme is a sort of reservoir engineering but is different from the other approaches [35–42], in that it relies on a reservoir composed of a series of dispersive and dissipative couplings, inspired by MF control composed of QND measurement and the subsequent filtering process.

The paper is organized as follows. In Sec. II, the CF-controller configuration is described in a general setting. Then we demonstrate how CF can replace MF for various state control problems: stabilization for a qubit (Sec. III) and qutrit (Sec. IV), spin squeezing (Sec. V), and Fock state generation (Sec. VI). Section VII concludes the paper.

II. THE CONTROLLER CONFIGURATION

For a general Markovian open quantum system interacting with a single probe field, the unconditional state obeys the master equation

$$\frac{d\rho}{dt} = -i[H,\rho] + L\rho L^\dagger - \frac{1}{2}L^\dagger L\rho - \frac{1}{2}\rho L^\dagger L. \quad (1)$$

Here L is the coupling operator and H is a Hamiltonian; see Appendix A for a detailed description of this equation. Thus, this system is generally characterized by (L,H). Let us consider two open systems $G_1 = (L_1,H_1)$ and $G_2 = (L_2,H_2)$ that are unidirectionally connected through a single probe field, as shown in Fig. 2(a). Then, under the assumption that the propagation time from G_1 to G_2 is negligible, the whole system, denoted as $G_1 \triangleright G_2$, behaves as a Markovian open system and is given by [23,43,44]

$$G_1 \triangleright G_2 = \left(L_1 + L_2, H_1 + H_2 + \frac{1}{2i}(L_2^\dagger L_1 - L_1^\dagger L_2)\right). \quad (2)$$

In this paper, we consider the case where L_1, L_2, H_1, and H_2 are operators living in the *same* Hilbert space associated with a single system. Then, as shown in Fig. 2(b), $G = G_1 \triangleright G_2$ is a CF-controlled system where the output field after the coupling
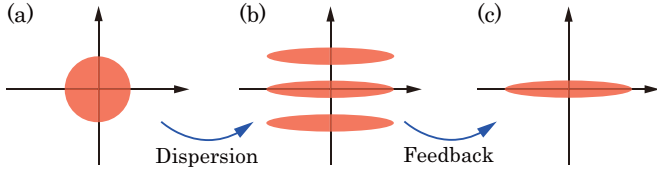
FIG. 1. Schematic of the feedback control for the case of squeezed state generation.

FIG. 3. (a) MF and (b) CF configuration for qubit control. (c) Fidelity $F = \langle\psi|\rho(\infty)|\psi\rangle$ between the ideal target state $|\psi\rangle$ and the steady state $\rho(\infty)$ in the realistic model.

L_1 is again coupled to the same system through L_2. Moreover, L_1 and L_2 are specified as follows. First, L_1 is Hermitian; $L_1 = L_1^\dagger$. This coupling induces a dispersive change of the system state depending on the field state. For the MF case, we measure the field after this coupling; then, ideally, the system's conditional state probabilistically changes toward one of the eigenstates of L_1, and a feedback control based on the measurement result compensates this randomness so that the target eigenstate is deterministically generated. Our CF strategy is to apply a fully quantum dissipative process that emulates this feedback operation; that is, in Fig. 2(b), L_2 is chosen as a dissipative coupling operator, which may drive the system state to the target. Summarizing, the CF-controlled system is given by

$$G = (L, H) = (e^{i\phi}L_1, H_{\text{sys}}) \triangleright (L_2, 0)$$

$$= \left(L_2 + e^{i\phi}L_1, H_{\text{sys}} + \frac{1}{2i}(e^{i\phi}L_2^\dagger L_1 - e^{-i\phi}L_1 L_2)\right), \quad (3)$$

where $L_1 = L_1^\dagger$ is a given dispersive coupling and L_2 is a dissipative one to be appropriately chosen. Also H_{sys} is a system Hamiltonian and $e^{i\phi}$ represents a phase shifter acting on the probe field. In what follows we demonstrate how to choose these operators and evaluate the performance of the resulting CF-controlled system, in some quantum control problems.

III. QUBIT STABILIZATION

In this section we study a qubit interacting with a probe field through the dispersive coupling operator $L_1 = \sqrt{\kappa}\sigma_z = \sqrt{\kappa}(|e\rangle\langle e| - |g\rangle\langle g|)$, where $|e\rangle = [1, 0]^\top$ and $|g\rangle = [0, 1]^\top$ [8,45–49]. If we continuously monitor the field after this coupling, as shown in Fig. 3(a), the qubit state conditioned on the measurement result probabilistically converges to $|e\rangle$ or $|g\rangle$; some MF controls compensate this random change and realize deterministic convergence to $|e\rangle$ or $|g\rangle$.

A. Control in the ideal setup

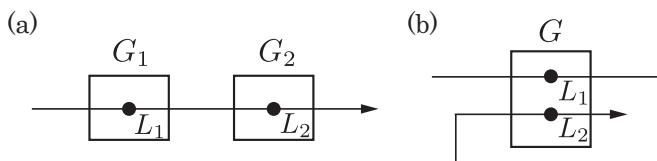First we study the CF control emulating the above MF scheme, in the ideal setting. Our initial task is to choose

FIG. 2. (a) Cascade connection of two open quantum systems G_1 and G_2. (b) CF for the system G via cascade connection.
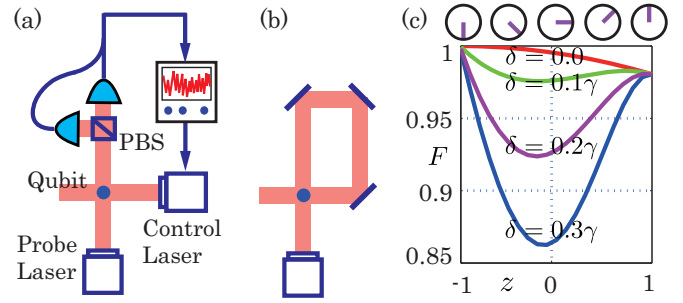
a suitable dissipative coupling L_2 that autonomously compensates the dispersive effect induced by L_1; here let us particularly take $L_2 = \sqrt{\gamma}\sigma_- = \sqrt{\gamma}|g\rangle\langle e|$, which represents the energy dissipation of a two-level atom with decay rate $\gamma > 0$. Figure 3(b) shows the configuration of this CF control; the qubit interacts with the field via L_1, and the output field is fed back to again couple to the system via L_2. Moreover we set $H_{\text{sys}} = 0$. Then the characteristic operators of this CF-controlled system (3) are given by

$$L = \sqrt{\gamma}\sigma_- + e^{i\phi}\sqrt{\kappa}\sigma_z = \begin{bmatrix} e^{i\phi}\sqrt{\kappa} & 0 \\ \sqrt{\gamma} & -e^{i\phi}\sqrt{\kappa} \end{bmatrix},$$

$$H = \frac{\sqrt{\kappa\gamma}}{2i}(e^{i\phi}\sigma_-^\dagger\sigma_z - e^{-i\phi}\sigma_z\sigma_-)$$

$$= \frac{\sqrt{\kappa\gamma}}{2i}\begin{bmatrix} 0 & -e^{i\phi} \\ e^{-i\phi} & 0 \end{bmatrix}. \quad (4)$$

Then, noting the fact that the uniqueness of the steady state for the general finite-dimensional master equation (1) is equivalent to the deterministic convergence to it [50], we find that any initial state $\rho(0)$ deterministically converges to the following steady state $\rho(\infty)$:

$$\rho(\infty) = |\psi\rangle\langle\psi|, \quad |\psi\rangle = \frac{1}{\sqrt{4\kappa + \gamma}}\begin{bmatrix} 2e^{i\phi}\sqrt{\kappa} \\ \sqrt{\gamma} \end{bmatrix}. \quad (5)$$

Interestingly, this is a *pure* state. Also, an *arbitrary* pure state, except $|e\rangle$, can be prepared by suitably choosing the control parameters γ and ϕ. $|e\rangle$ can be approximately generated by setting $\gamma \ll \kappa$, although we should note that the dispersive coupling is usually realized in the so-called weak-coupling regime where κ is relatively small. Recall now that the MF control can exactly stabilize $|e\rangle$ in an ideal setup, while it cannot stabilize any pure state other than $|e\rangle$ and $|g\rangle$. Hence, this CF is not a control scheme that outperforms MF. Rather, the important fact we have learned through this case study is that the CF scheme certainly has an ability to emulate the functionality of MF, i.e., the ability to compensate the dispersion effect by autonomous dissipation and as a result generate a desired unconditional state.

Before closing this subsection, we provide another way to prove the unique convergence of the CF-controlled system to the state $|\psi\rangle$ given by Eq. (5). We use the following theorem.

Theorem 1 [51,52]. A pure state $|\Psi\rangle$ is a steady state of the master equation (1) if and only if $|\Psi\rangle$ is a common eigenvector of L and $iH + L^\dagger L/2$.

Now the eigenvectors of the operator L are given by $|g\rangle$ and $|\psi\rangle$. Then it is immediate to see that $|\psi\rangle$ is an eigenvector of

$$iH + \frac{1}{2}L^\dagger L = \begin{bmatrix} (\kappa + \gamma)/2 & -e^{i\phi}\sqrt{\kappa\gamma} \\ 0 & \kappa/2 \end{bmatrix},$$

but $|g\rangle$ is not. Thus, from the above theorem, $|\psi\rangle$ is a *unique* steady state; actually, if there exists a *mixed* steady state, then $|g\rangle$ must also be a steady state due to the convexity of the Bloch sphere, which is a contradiction. As a result, any initial state $\rho(0)$ converges to $|\psi\rangle$.

Remark 1. Let us consider the setup where the two couplings occur in a wrong order; that is, the field first couples with the system via the dissipative operator $L_1 = \sqrt{\gamma}\sigma_-$ and secondly with the dispersive one $L_2 = \sqrt{\kappa}\sigma_z$ in the feedback way. Then the operators of the CF-controlled system are given by

$$L = \sqrt{\kappa}\sigma_z + e^{i\phi}\sqrt{\gamma}\sigma_- = \begin{bmatrix} \sqrt{\kappa} & 0 \\ e^{i\phi}\sqrt{\gamma} & -\sqrt{\kappa} \end{bmatrix},$$

$$H = \frac{\sqrt{\kappa\gamma}}{2i}(e^{i\phi}\sigma_z\sigma_- - e^{-i\phi}\sigma_-^\dagger\sigma_z) = \frac{\sqrt{\kappa\gamma}}{2i}\begin{bmatrix} 0 & e^{i\phi} \\ -e^{-i\phi} & 0 \end{bmatrix}.$$

In this case, the ground state $|g\rangle = [0,1]^\top$ is the unique steady state of the master equation; hence any initial state converges to $|g\rangle$. This is a reasonable result, because what the CF controller considered here is doing is to emulate the operation such that the stabilizing control for $|g\rangle$ is performed *before* the measurement. Therefore, though not useful, this result also shows the fact that the all-quantum CF scheme certainly has an ability to emulate the measurement feedback operation.

B. Control performance in the imperfect setting

To demonstrate the control performance of the proposed CF scheme in a realistic situation, here we consider the setup of circuit QED [45]; this paper presented a method for continuously monitoring a superconducting charge qubit that dispersively couples to a transmission line resonator. The master equation for the CF-controlled qubit, which takes into account the imperfections studied in [45], is given by

$$\frac{d\rho}{dt} = -i[H + H_\delta, \rho] + \mathcal{D}[L]\rho + \mathcal{D}[L_{\text{ex}}^{(1)}]\rho + \mathcal{D}[L_{\text{ex}}^{(2)}]\rho, \tag{6}$$

where H and L are the operators in the ideal setting given in Eq. (4). That is, in the practical situation, the qubit system is driven by the external Hamiltonian $H_\delta = \delta\sigma_z$ with δ the detuning between the qubit transition frequency and the driving probe frequency. Moreover, the system is coupled to another uncontrollable dissipative channel characterized by the Lindblad operator $L_{\text{ex}}^{(1)} = \sqrt{\epsilon_1}\sigma_-$ and further a dephasing channel $L_{\text{ex}}^{(2)} = \sqrt{\epsilon_2}\sigma_z$. In the recent experimental study [49], which has applied the theory of [45] to perform the MF control for qubit state preparation, the system parameters are $\kappa/2\pi = 0.13$ MHz and $\epsilon_2/2\pi = 0.005$ MHz; hence $\epsilon_2 \approx 0.04\kappa$, meaning that roughly 4% loss occurs in the dispersive coupling process. We expect further progress will be made in experiments and assume $\epsilon_2 = 0.01\kappa$ in the simulation. Also

we set $\epsilon_1 = 0.01\gamma$, i.e., 1% loss in the dissipative coupling process. Finally $\phi = 0$ is chosen for simplicity. Figure 3(c) shows the fidelity between the target state $|\psi\rangle$ in Eq. (5) with $\phi = 0$ and the steady state $\rho(\infty)$ of the master equation (6), as a function of the z component of the Bloch vector corresponding to $|\psi\rangle$ [the target Bloch vector is depicted for several z in the top of Fig. 3(c)]. Note that, from the equation

$$|\psi\rangle\langle\psi| = \frac{1}{4\kappa + \gamma}\begin{bmatrix} 4\kappa & 2\sqrt{\kappa\gamma} \\ 2\sqrt{\kappa\gamma} & \gamma \end{bmatrix} = \frac{1}{2}\begin{bmatrix} 1 + z & x \\ x & 1 - z \end{bmatrix},$$

we have $z = (4\kappa/\gamma - 1)/(4\kappa/\gamma + 1)$. In the ideal setting (the case $\delta = 0$, $\epsilon_1 = 0$, and $\epsilon_2 = 0$), the fidelity takes $F(z) = \langle\psi|\rho(\infty)|\psi\rangle = 1$ for all z; that is, as proven in the previous subsection, an arbitrary pure qubit state (except $|e\rangle$) can be prepared by suitably choosing the system parameter κ/γ. In the practical setting, if the detuning δ is small (desirably the case $\delta = 0$ in the figure), the fidelity monotonically decreases as z increases, due to the additional decoherence process $L_{\text{ex}}^{(1)} = \sqrt{0.01\gamma}\sigma_-$ and $L_{\text{ex}}^{(2)} = \sqrt{0.01\kappa}\sigma_z$. The figure shows that, in this case, states close to the ground state can be prepared with good fidelity nearly $F(z) \approx 1$. In particular, the superposition $(|g\rangle + |e\rangle)/\sqrt{2}$ can be stabilized with fidelity bigger than 0.99. On the other hand, if δ becomes large, the fidelity function takes the minimum at around $z = -0.1$ and decreases down to about 0.86 when $\delta = 0.3\gamma$. It is notable, however, that even in those cases a state close to the excited state can be produced with fidelity $\approx$0.97. Therefore, the CF scheme functions as a robust emulator for selectively producing $|e\rangle$ or $|g\rangle$. Note of course that, in order to stabilize a superposition, the detuning should be sufficiently suppressed.

IV. QUTRIT STABILIZATION

Next, let us consider a qutrit such as a three-level atom, with states $|1\rangle = [1,0,0]^\top$, $|2\rangle = [0,1,0]^\top$, and $|3\rangle = [0,0,1]^\top$. We assume that the following dispersive coupling L_1 and the dissipative one L_2 can be implemented [53,54]:

$$L_1 = \sqrt{\kappa}\begin{bmatrix} 1 & 0 & 0 \\ 0 & 0 & 0 \\ 0 & 0 & -1 \end{bmatrix}, L_2 = \sqrt{\gamma}\begin{bmatrix} 0 & 0 & 0 \\ 1 & 0 & 0 \\ 0 & 1 & 0 \end{bmatrix}.$$

Measuring the probe after the dispersive coupling L_1 produces the conditional state, which probabilistically converges to one of the eigenstates of $L_1, \{|1\rangle, |2\rangle, |3\rangle\}$; a suitable MF control can compensate this dispersive change and deterministically stabilize an arbitrary eigenstate [12,13]. As for L_2, this induces the state change $|1\rangle \rightarrow |2\rangle \rightarrow |3\rangle$, i.e., a ladder-type dissipation for a three-level atom illustrated in Fig. 4(a). This dissipation is induced by the coupling of the qutrit to a single probe field $B(t)$; the Hamiltonian representing this instantaneous coupling is given by (see Appendix A)

$$H_{\text{int}}(t + dt, t) = i\sqrt{\gamma}(|3\rangle\langle 2| + |2\rangle\langle 1|)dB^\dagger(t) + \text{H.c.}$$

A. Control in the ideal setup

First let us set $H_{\text{sys}} = 0$ and $\phi = 0$. Then the CF-controlled system (3), which might be implemented in a similar setup as
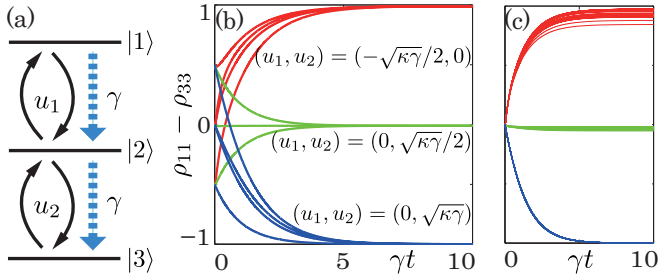
FIG. 4. (a) Energy diagram of the states and time evolution of $\rho_{11} - \rho_{33}$ in the case $\kappa = 100\gamma$, (b) with several initial states in the ideal setup and (c) with a specific initial state in the realistic setup.

Fig. 3(b), is characterized by

$$
L = \begin{bmatrix} \sqrt{\kappa} & 0 & 0 \\ \sqrt{\gamma} & 0 & 0 \\ 0 & \sqrt{\gamma} & -\sqrt{\kappa} \end{bmatrix}, \quad H = \frac{i\sqrt{\kappa\gamma}}{2} \begin{bmatrix} 0 & 0 & 0 \\ 0 & 0 & 1 \\ 0 & -1 & 0 \end{bmatrix}.
$$
(7)

The master equation has the following unique solution:

$$
\rho(\infty) = \frac{1}{5\kappa + \gamma} \begin{bmatrix} 0 & 0 & 0 \\ 0 & 4\kappa & 2\sqrt{\kappa\gamma} \\ 0 & 2\sqrt{\kappa\gamma} & \kappa + \gamma \end{bmatrix}.
$$

Unlike the qubit case, this is not a pure state; purity is $\mathrm{Tr}[\rho(\infty)^2] = 1 - 8/(5 + \gamma/\kappa)^2$. For instance when $\gamma = 3\kappa$, $\rho(\infty)$ approximates $|\Psi_{23}\rangle = (|2\rangle + |3\rangle)/\sqrt{2}$ with fidelity $\langle\Psi_{23}|\rho(\infty)|\Psi_{23}\rangle \approx 9.33$. However, $\rho(\infty)$ is a particular mixed state, which can stabilize neither $|1\rangle$ nor $|2\rangle$.

To emulate the MF scheme and stabilize an arbitrary eigenstate of L_1, the CF scheme needs to have a system Hamiltonian H_{sys} to move the steady state. Here we take

$$
H_{\mathrm{sys}} = iu_1(|2\rangle\langle 1| - |1\rangle\langle 2|) + iu_2(|3\rangle\langle 2| - |2\rangle\langle 3|), \quad (8)
$$

where (u_1, u_2) are real parameters to be determined; H_{sys} exchanges $|1\rangle$ and $|2\rangle$ with strength u_1, and $|2\rangle$ and $|3\rangle$ with u_2 as shown in Fig. 4(a). Finally we set $\phi = 0$. Then the CF-controlled system (3) is characterized by L in Eq. (7) and

$$
H = \begin{bmatrix} 0 & -iu_1 & 0 \\ iu_1 & 0 & -iu_2 + i\sqrt{\kappa\gamma}/2 \\ 0 & iu_2 - i\sqrt{\kappa\gamma}/2 & 0 \end{bmatrix}. \quad (9)
$$

The parameter (u_1, u_2) can be determined by using Theorem 1 given in Sec. III A. Now, the eigenvectors of L are calculated as

$$
|\Phi_1\rangle = \frac{1}{2\kappa + \gamma} \begin{bmatrix} 2\kappa \\ 2\sqrt{\kappa\gamma} \\ \gamma \end{bmatrix}, \quad |\Phi_2\rangle = \frac{1}{\sqrt{\kappa + \gamma}} \begin{bmatrix} 0 \\ \sqrt{\kappa} \\ \sqrt{\gamma} \end{bmatrix},
$$

and $|\Phi_3\rangle = |3\rangle$. Note that, if $\kappa \gg \gamma$, $|\Phi_1\rangle$ and $|\Phi_2\rangle$ approximate $|1\rangle$ and $|2\rangle$, respectively. Then, by solving the equation $(iH + L^\dagger L/2)|\Phi_j\rangle = \lambda_j|\Phi_j\rangle$, we end up with $(u_1, u_2) = (-\sqrt{\kappa\gamma}/2, 0)$ for the case $|\Phi_1\rangle$, $(u_1, u_2) = (0, \sqrt{\kappa\gamma}/2)$ for the case $|\Phi_2\rangle$, and $u_2 = \sqrt{\kappa\gamma}$ for the case $|\Phi_3\rangle$. Moreover, each $|\Phi_j\rangle$ is a *unique* steady state of the CF-controlled system (the proof is given in Appendix B), and thus any $\rho(0)$ converges to $|\Phi_j\rangle$ according to the result of [50].

In Fig. 4(b) the time evolution of $\rho_{11} - \rho_{33}$ is plotted with several initial states $\rho(0)$ in the ideal setup. The parameters are taken as $\kappa = 100\gamma$, hence $|\Phi_1\rangle \approx |1\rangle$ and $|\Phi_2\rangle \approx |2\rangle$. This figure shows that, by properly choosing the control parameters (u_1, u_2), we can selectively and deterministically generate $|1\rangle$, $|2\rangle$, or $|3\rangle$. (Note that $\rho_{11} - \rho_{33} \to 0$ indicates $\rho \to |2\rangle\langle 2|$ in the figure.) That is, the CF scheme certainly emulates the corresponding MF control.

B. Control performance in the imperfect setting

Here we study a three-level artificial ladder-type atom implemented in a superconducting circuit [54], as a realistic model of the qutrit system. The first practical imperfection is the parameter mismatch. Recall that we need to add the driving Hamiltonian H_{sys}, and its parameters have to be exactly specified. For instance, if $|\Phi_1\rangle$ is the target, then the parameters must be exactly $(u_1, u_2) = (-\sqrt{\kappa\gamma}/2, 0)$. In reality, however, there exists a deviation:

$$
u_1 = -(1 + \Delta)\sqrt{\kappa\gamma}/2,
$$

where Δ is the unknown parameter. Similarly, $u_2 = (1 + \Delta)\sqrt{\kappa\gamma}/2$ for the case of $|\Phi_2\rangle$ and $u_2 = (1 + \Delta)\sqrt{\kappa\gamma}$ for the case of $|\Phi_3\rangle$. The nonzero Δ would affect the performance of control.

Next, in addition to the driving Hamiltonian H_{sys} given by Eq. (8), the system is subjected to

$$
H_\delta = \delta_1|1\rangle\langle 1| + \delta_2|2\rangle\langle 2|,
$$

where $\delta_1 = \omega_{13} - \omega_{\mathrm{in}} - \Omega_1$ and $\delta_2 = \omega_{23} - \omega_{\mathrm{in}} - \Omega_2$ are detunings; ω_{13} and ω_{23} are the transition frequency of the energy levels $|1\rangle \leftrightarrow |3\rangle$ and $|2\rangle \leftrightarrow |3\rangle$, respectively, with ω_{in} the center frequency of the probe input field and Ω_i the frequency of the driving Hamiltonian with strength u_i. As in the case of parameter mismatch, the detunings also violate the condition for the system to have a pure steady state.

The last imperfection is decoherence. In addition to the ideal ladder-type decay process represented by L_2, in reality there exist independent decay processes such that the emitted photon leaks to the fields $B_1(t)$ and $B_2(t)$. This coupling is represented by the interaction Hamiltonian

$$
H'_{\mathrm{int}}(t + dt, t) = i\sqrt{\epsilon_1}[|2\rangle\langle 1|dB_1^\dagger(t) - |1\rangle\langle 2|dB_1(t)]
$$
$$
+ i\sqrt{\epsilon_2}[|3\rangle\langle 2|dB_2^\dagger(t) - |2\rangle\langle 3|dB_2(t)].
$$

The master equation of the CF-controlled system, which takes into account the above imperfections, is

$$
\frac{d\rho}{dt} = -i[H + H_\delta, \rho] + \mathcal{D}[L]\rho + \mathcal{D}[L_{\mathrm{ex}}^{(1)}]\rho + \mathcal{D}[L_{\mathrm{ex}}^{(2)}]\rho,
$$

where $L_{\mathrm{ex}}^{(1)} = \sqrt{\epsilon_1}|2\rangle\langle 1|$, $L_{\mathrm{ex}}^{(1)} = \sqrt{\epsilon_2}|3\rangle\langle 2|$, L in Eq. (7), and H in Eq. (9). The simulation shown in Fig. 4(c) has been carried out with the following parameter choice. First we take $\kappa = 100\gamma$, which realizes $|\Phi_1\rangle \approx |1\rangle$ and $|\Phi_2\rangle \approx |2\rangle$. In the ideal case where $\Delta, \delta_1, \delta_2, \epsilon_1$, and ϵ_2 are all zero, the qutrit state $\rho(t)$ selectively converges to one of $\{|1\rangle, |2\rangle, |3\rangle\}$, as demonstrated in Fig. 4(b). The decoherence strength is fixed to $\epsilon_1 = \epsilon_2 = \sqrt{\kappa\gamma}/1000$, in view of the fact that, in the experiment [54], the corresponding parameters are estimated as $\epsilon = 2\pi \times 0.272$ MHz and $\sqrt{\kappa\gamma} = 2\pi \times 240$ MHz. For

the detunings (δ_1, δ_2), they take random numbers generated from the uniformly random distribution on $[-\sqrt{\kappa\gamma}, \sqrt{\kappa\gamma}]$. The parameter uncertainty Δ also takes a random number generated from the uniformly random distribution on $[-0.01, 0.01]$. The random variables $(\delta_1, \delta_2, \Delta)$ are independent. The simulation result with this setting is depicted in Fig. 4(c), where for each case of $|\Phi_i\rangle$ 30 sample paths are plotted. This figure clearly shows that the state convergence to $|2\rangle$ or $|3\rangle$ is robust against the above imperfections. For the case of $|1\rangle$, it seems that the fluctuation of the trajectories is not small, but the mean value of the fidelity $\langle 1|\rho(\infty)|1\rangle$ is 0.9531. Therefore, we can conclude that the CF-control scheme functions as a robust state generator.

Remark 2. The robustness property against the detuning H_δ can be theoretically explained as follows, especially when $\epsilon_1 = \epsilon_2 = \Delta = 0$. The iff condition for the pure state $|\Phi_i\rangle$ to be a steady state is that it is an eigenvector of $i(H + H_\delta) + L^\dagger L/2$; in the case of $|\Phi_1\rangle$, this condition is represented by

$$
\begin{bmatrix} i\delta_1 + (\kappa + \gamma)/2 & u_1 & 0 \\ -u_1 & i\delta_2 + \gamma/2 & u_2 - \sqrt{\kappa\gamma} \\ 0 & -u_2 & \kappa/2 \end{bmatrix} \begin{bmatrix} 2\kappa \\ 2\sqrt{\kappa\gamma} \\ \gamma \end{bmatrix}
$$
$$
= \begin{bmatrix} 2i\kappa\delta_1 + \kappa(\kappa + \gamma) + 2u_1\sqrt{\kappa\gamma} \\ -2u_1\kappa + 2i\delta_2\sqrt{\kappa\gamma} + \gamma u_2 \\ -2u_2\sqrt{\kappa\gamma} + \kappa\gamma/2 \end{bmatrix} = \lambda \begin{bmatrix} 2\kappa \\ 2\sqrt{\kappa\gamma} \\ \gamma \end{bmatrix},
$$

for some constant λ. Now we choose $(u_1, u_2) = (-\sqrt{\kappa\gamma}/2, 0)$, which are the optimal parameters in the ideal case $\delta_1 = \delta_2 = 0$. Then, the above eigenequation becomes

$$
\begin{bmatrix} \kappa^2 + 2i\kappa\delta_1 \\ \kappa\sqrt{\kappa\gamma} + 2i\delta_2\sqrt{\kappa\gamma} \\ \kappa\gamma/2 \end{bmatrix} = \lambda \begin{bmatrix} 2\kappa \\ 2\sqrt{\kappa\gamma} \\ \gamma \end{bmatrix},
$$

which approximately holds with $\lambda = \kappa/2$, if δ_1 and δ_2 are much smaller than κ. Hence, $|\Phi_1\rangle$ is a robust steady state of the CF-controlled system, under the influence of the detuning. Likewise, we can prove the robustness property of $|\Phi_2\rangle$ and $|\Phi_3\rangle$.

V. SPIN SQUEEZING

We next study an atomic ensemble. The goal is to generate a spin-squeezed state, which can be applied for quantum magnetometry [56]. The basic variables are the spin angular momentum operators (J_x, J_y, J_z). They satisfy $[J_x, J_y] = iJ_z$ and accordingly $\langle \Delta J_x^2 \rangle \langle \Delta J_y^2 \rangle \geqslant |\langle J_z \rangle|^2/4$, where $\langle J_i \rangle = \mathrm{Tr}(J_i \rho)$ and $\Delta J_i = J_i - \langle J_i \rangle$. Also the lowering operator is defined as $J_- = J_x - iJ_y$. Here we assume that the ensemble is large, i.e., $J \gg 1$, and the state lies near the collective spin-down state. Then J_z can be approximated as $J_z \approx -J$, and (J_x, J_y) satisfy $[J_x, J_y] = -iJ$ and thus $\langle \Delta J_x^2 \rangle \langle \Delta J_y^2 \rangle \geqslant J^2/4$. Hence the spin operators can be transformed to the boson operators as $q = J_x/\sqrt{J}$, $p = -J_y/\sqrt{J}$, and $a = (q + ip)/\sqrt{2} = J_-/\sqrt{2J}$ [55]. As shown in Fig. 5, this is a projection from the generalized Bloch sphere onto the two-dimensional phase space.

Suppose that the atomic ensemble dispersively couples with an optical field with annihilation operator $B_1(t)$ via the
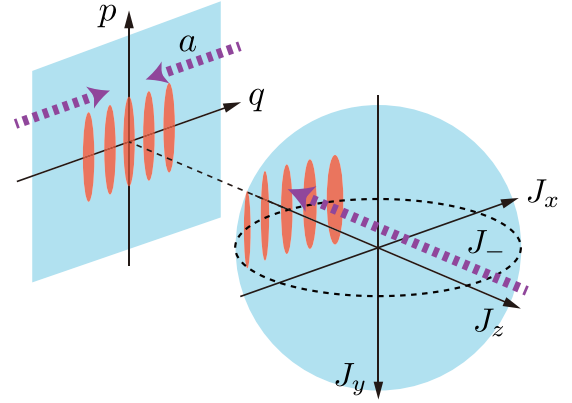

FIG. 5. Projection of the spin operators to the boson operators, for a large atomic ensemble.

following Faraday interaction Hamiltonian [7,18,19]:

$$
H_{\mathrm{int}}^{(1)}(t + dt, t) = i\sqrt{\kappa}[q \, dB_1^\dagger(t) - q \, dB_1(t)],
$$

meaning that $L_1 = \sqrt{\kappa} q$. Through this interaction, the polarization of the optical probe field changes depending on the system's energy level. Hence, measuring the probe field after this coupling yields the conditional squeezed state with random amplitude on the q axis as shown in Fig. 5; then, as implied by Fig. 1, a suitable MF can compensate this dispersive change and generate an unconditional squeezed vacuum state. Here we take the following dissipative system-field coupling, which simply represents the energy decay, to construct a CF that emulates this MF control:

$$
H_{\mathrm{int}}^{(2)}(t + dt, t) = i\sqrt{\gamma}[a \, dB_2^\dagger(t) - a^\dagger \, dB_2(t)],
$$

meaning that $L_2 = \sqrt{\gamma} a$. In fact, as indicated by the purple arrows in Fig. 5, this dissipative CF operation will stabilize a squeezed vacuum state, or equivalently a spin squeezed state at around $J_z \approx -J$. This means that an additional system Hamiltonian would not be necessary to achieve the goal; that is, $H_{\mathrm{sys}} = 0$. Also we set $\phi = 0$. Then the system operators of the CF-controlled system (3) are given by

$$
H = \frac{1}{2i}(L_2^\dagger L_1 - L_1^\dagger L_2) = -\frac{\sqrt{\kappa\gamma}}{2}(qp + pq),
$$
$$
L = L_1 + L_2 = (\sqrt{\kappa} + \sqrt{\gamma})q + i\sqrt{\gamma} p.
$$

Note that $H \propto J_x J_y + J_y J_x$ is the two-axis twisting Hamiltonian [56], which itself has an ability to yield a spin squeezed state. As noted in Sec. I, there are several approaches for producing such a squeezing operation via CF [35–39,41,42], but the method proposed in this paper differs from those in that it utilizes a feedback operation composed of a series of dispersive and dissipative couplings inspired by the corresponding MF control.

Now, $\rho(t)$ is Gaussian for all t, and thus it can be fully characterized by the mean vector $\langle x \rangle = [\langle q \rangle, \langle p \rangle]^\top$ and the covariance matrix

$$
V = \begin{bmatrix} \langle \Delta q^2 \rangle & \langle \Delta q \Delta p + \Delta p \Delta q \rangle/2 \\ \langle \Delta q \Delta p + \Delta p \Delta q \rangle/2 & \langle \Delta p^2 \rangle \end{bmatrix},
$$

where $\Delta q = q - \langle q \rangle$ and $\Delta p = p - \langle p \rangle$. These statistical variables are subjected to the equations $d\langle x \rangle/dt = A\langle x \rangle$ and

$dV/dt = AV + VA^\top + D$, where

$$A = \begin{bmatrix} -2\sqrt{\kappa\gamma} - \gamma & 0 \\ 0 & -\gamma \end{bmatrix}, D = \begin{bmatrix} \gamma & 0 \\ 0 & (\sqrt{\kappa} + \sqrt{\gamma})^2 \end{bmatrix}.$$

The derivation of these matrices is given in Appendix C. Then, in the limit $t \to \infty$, $\langle x(t) \rangle \to 0$ and $V(t)$ converges to the diagonal matrix $\mathrm{diag}(\langle \Delta q(\infty)^2 \rangle, \langle \Delta p(\infty)^2 \rangle)$ with

$$\langle \Delta q(\infty)^2 \rangle = \frac{\sqrt{\gamma}}{4\sqrt{\kappa} + 2\sqrt{\gamma}}, \quad \langle \Delta p(\infty)^2 \rangle = \frac{(\sqrt{\kappa} + \sqrt{\gamma})^2}{2\gamma}.$$

Clearly, $\langle \Delta q(\infty)^2 \rangle < 1/2$, hence the squeezed state is generated by the CF control. For example when $\kappa = 9\gamma$, the variances are $\langle \Delta q(\infty)^2 \rangle = 1/14$ and $\langle \Delta p(\infty)^2 \rangle = 8$, which corresponds to about 8.5-dB squeezing. In this case the purity is only $\mathrm{Tr}[\rho(\infty)^2] = 1/\sqrt{4\det[V(\infty)]} \approx 0.66$, but this would not be a serious issue for the application to quantum metrology.

Remark 3. Let us consider the setup where the two system-probe couplings occur in the wrong order along the feedback loop; the dissipative coupling represented by $L_1 = \sqrt{\gamma}a$ first occurs, and secondly the dispersive one $L_2 = \sqrt{\kappa}q$ occurs. In this case, the Hamiltonian is calculated as $H = \sqrt{\kappa\gamma}(qp + pq)/2$. The coupling operator is the same as before, i.e., $L = L_1 + L_2 = \sqrt{\gamma}a + \sqrt{\kappa}q$. Then the system matrices characterizing this linear system are given by

$$A = \begin{bmatrix} -\gamma & 0 \\ 0 & -\gamma - 2\sqrt{\kappa\gamma} \end{bmatrix}, D = \begin{bmatrix} \gamma & 0 \\ 0 & (\sqrt{\kappa} + \sqrt{\gamma})^2 \end{bmatrix}.$$

Then, the steady covariance matrix of the dynamics $dV/dt = AV + VA^\top + D$ is obtained as

$$V(\infty) = \frac{1}{2}\begin{bmatrix} 1 & 0 \\ 0 & 1 + \kappa/(\gamma + 2\sqrt{\kappa\gamma}) \end{bmatrix}.$$

Hence, the steady state is not a squeezed state. Note that, as in the qubit case discussed in Remark 1, this results emphasizes the importance of the ordering of the two couplings.

VI. FOCK STATE GENERATION

Lastly we consider the problem for generating a Fock state via feedback. The system is a high-Q optical cavity containing a few photons. In Refs. [9–11], the dispersive coupling $L_1 = \sqrt{\kappa}n$, where $n = a^\dagger a$ with a the annihilation operator of the cavity mode, was taken for MF control; this is the cross Kerr coupling between the cavity field and the probe field represented by B_1, the instantaneous Hamiltonian of which is given by

$$H_{\mathrm{int}}^{(1)}(t + dt, t) = i\sqrt{\kappa}[n dB_1^\dagger(t) - n dB_1(t)].$$

In fact, this coupling induces a phase shift on B_1 depending on the number of photons inside the cavity; hence, by measuring the output field represented by $d\tilde{B}_1(t) = \sqrt{\kappa}j_t(n)dt + dB_1(t)$ [see Eq. (A5)], we can estimate the number of cavity photons and probabilistically obtain one of the eigenstates of L_1, i.e., a conditional Fock state $|m\rangle$.

Our aim is to construct a dissipative CF controller that compensates the dispersive process L_1 and produces a target Fock state deterministically. A simple dissipative process is the optical decay $L_2 = \sqrt{\gamma}a$, represented by the interaction
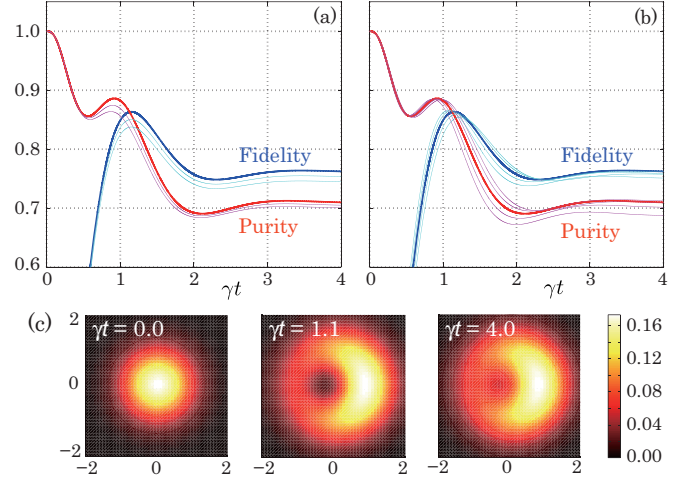

FIG. 6. (a, b) Time evolution of the fidelity $F(t) = \langle 1|\rho(t)|1\rangle$ and the purity $P(t) = \mathrm{Tr}(\rho(t)^2)$; the solid red and blue lines are the case of ideal setup, while cyan and magenta lines are the case under (a) decoherence and (b) parameter mismatch. (c) Q function of the system state at $\gamma t = 0, 1.1, 4.0$ in the ideal setting.

Hamiltonian

$$H_{\mathrm{int}}^{(2)}(t + dt, t) = i\sqrt{\gamma}[a dB_2^\dagger(t) - a^\dagger dB_2(t)],$$

where $B_2(t)$ is the annihilation field operator of the corresponding optical field. The CF control is structured by connecting the output $\tilde{B}_1$ to the input B_2.

Moreover, we add a displacement Hamiltonian $H_{\mathrm{sys}} = ig(a^\dagger - a)$, where g is the gain to be determined, to move the steady state; note that merely the vacuum is produced if $H_{\mathrm{sys}} = 0$. Also we take $\phi = 0$. Hence, the CF-controlled system (3) is characterized by

$$L = \sqrt{\kappa}n + \sqrt{\gamma}a, H = ig(a^\dagger - a) + \frac{\sqrt{\kappa\gamma}}{2i}(a^\dagger n - na). \tag{10}$$

Now we fix the target to the single-photon $|1\rangle$, with initial state $\rho(0) = |0\rangle\langle 0|$. The control parameters are $\gamma = \kappa/4$ and $g = \kappa/2$, which are chosen to maximize the fidelity $F(t) = \langle 1|\rho(t)|1\rangle$, at some point of time t. The blue and red lines in Figs. 6(a) and 6(b) show the time evolution of $F(t)$ and the purity $P(t) = \mathrm{Tr}[\rho(t)^2]$, respectively; the maximum fidelity is $F \approx 0.86$ at $\gamma t = 1.1$ (with $P \approx 0.86$), and $F(t)$ converges to $F \approx 0.76$ (with $P \approx 0.71$). Therefore, the proposed CF controller actually emulates the MF scheme and generates a state close to $|1\rangle$ before reaching the steady state which still has a feature of $|1\rangle$, as indicated by the Q function $Q(\alpha) = \langle\alpha|\rho|\alpha\rangle/\pi$ shown in Fig. 6(c).

We also should study the effect of imperfection. In practice, there exists an uncontrollable photon leakage; we model this imperfection by introducing an extra optical field B_3 coupled to the cavity through the interaction Hamiltonian

$$H_{\mathrm{int}}^{(3)}(t + dt, t) = i\sqrt{\epsilon}[a dB_3^\dagger(t) - a^\dagger dB_3(t)].$$

The master equation of the CF-controlled system is then given by

$$\frac{d\rho}{dt} = -i[H, \rho] + \mathcal{D}[L]\rho + \mathcal{D}[L_{\mathrm{ex}}]\rho, \quad L_{\mathrm{ex}} = \sqrt{\epsilon}a,$$

with (L, H) given in Eq. (10). In Ref. [9] the author estimated $\epsilon = 12$ kHz while $\kappa = 2.5$ MHz, which leads to $\epsilon \approx \kappa/200$; hence we take $\epsilon = \kappa/50, \kappa/100$. The cyan and magenta lines in Fig. 6(a) represent $F(t)$ and $P(t)$, respectively, in this imperfect setting. The figure shows that the peak fidelity $F(t) = \langle 1|\rho(t)|1\rangle$ at $\gamma t = 1.1$ decreases from the optimal value 0.86 to 0.84. Apart from the decoherence, we have studied the case where the gain parameter g in the displacement operation $ig(a^\dagger - a)$ deviates from the optimal value $g = \kappa/2$. Figure 6(b) shows the case $g = \kappa/2 + \Delta$ with $\Delta = \pm\kappa/40, \pm\kappa/80$, while $\epsilon = 0$ is assumed. Then from the figure we find that the fluctuation of the peak fidelity at $\gamma t = 1.1$ is smaller than the case of decoherence. In summary, in both cases (a, b), the performance degradation is not so big, hence the CF scheme for the single-photon generation is robust against those practical imperfections. This is in stark contrast to the MF strategy [14] where $|1\rangle$ is generated with fidelity $F \approx 0.9$ but is collapsed immediately.

VII. CONCLUSION

In this paper we demonstrated that a CF control can replace the MF one for the purpose of state preparation in some typical settings. The CF controller has a common structure, which is simply a series of dispersive and dissipative couplings inspired by the corresponding MF operation. Hence, it would have a wide applicability in practice and work for other important objectives such as the quantum error correction. In fact, some studies along this direction have been conducted in a particular setup [57,58]. The sophisticated design theory for dissipative quantum networks [59] would be useful to solve those problems.

ACKNOWLEDGMENTS

APPENDIX A: MARKOVIAN OPEN QUANTUM SYSTEMS

1. Quantum stochastic differential equation and master equation

Here we derive the dynamical equation and the master equation of a general Markovian open quantum system that interacts with a single coherent field.

Let $b(t)$ be the annihilation operator of the coherent field and assume that $b(t)$ instantaneously interacts with the system. $b(t)$ satisfies the canonical commutation relation $[b(t), b^\dagger(s)] = \delta(t - s)$. As in the classical case, such a white-noise process can be rigorously treated by introducing the annihilation process operator $B(t) = \int_0^t b(s)ds$; in particular, the infinitesimal change $dB(t) = B(t + dt) - B(t)$ satisfies the following *quantum Ito rule* [44]:

$$dt\, dB = 0, \quad dB\, dB^\dagger = dt, \quad dB^2 = (dB^\dagger)^2 = dB^\dagger dB = 0.$$
(A1)

The system-field interaction in the short time interval $[t, t + dt]$ is generally described by the Hamiltonian

$$H_{\text{int}}(t + dt, t) = i[L\, dB^\dagger(t) - L^\dagger dB(t)],$$
(A2)

where L is a system operator representing the coupling with the field. The corresponding unitary operator in this time interval is given by $U(t + dt, t) = \exp[-iH_{\text{int}}(t + dt, t)]$. Then the total unitary operator from time zero to t, denoted by $U(t)$, is constructed by $U(t + dt) = U(t + dt, t)U(t)$, and from the quantum Ito rule (A1) we can derive the time evolution of $U(t)$ as follows:

$$U(t + dt)$$
$$= \exp[-iH\,dt - iH_{\text{int}}(t + dt, t)]U(t)$$
$$= \left[I - iH\,dt - iH_{\text{int}}(t + dt, t) - \tfrac{1}{2}H_{\text{int}}(t + dt, t)^2\right]U(t)$$
$$= \left[I - \left(iH + \tfrac{1}{2}L^\dagger L\right)dt + L\,dB^\dagger(t) - L^\dagger dB(t)\right]U(t),$$
(A3)

with $U(0) = I$, where we have added the time-invariant system Hamiltonian H [thus, the total Hamiltonian is $H\,dt + H_{\text{int}}(t + dt, t)$]. From $dU(t) = U(t + dt) - U(t)$, Eq. (A3) is equivalently represented by

$$dU(t) = \left[-\left(iH + \tfrac{1}{2}L^\dagger L\right)dt + L\,dB^\dagger(t) - L^\dagger dB(t)\right]U(t),$$

with $U(0) = I$. This is called the quantum stochastic differential equation (QSDE). Thus, a Markovian open quantum system G, which interacts with a single coherent field, is generally characterized by two operators L and H, and thus it is denoted by $G = (L, H)$.

For an arbitrary system operator X, the Heisenberg equation of $X(t) = j_t(X) = U^\dagger(t)XU(t)$ is given by

$$= U^\dagger(t + dt)XU(t + dt) - U^\dagger(t)XU(t)$$
$$= dU^\dagger(t)XU(t) + U^\dagger(t)X\,dU(t) + dU^\dagger(t)X\,dU(t)$$
$$= j_t\left(i[H, X] + L^\dagger XL - \tfrac{1}{2}L^\dagger LX - \tfrac{1}{2}XL^\dagger L\right)dt$$
$$\quad + j_t([X, L])dB^\dagger(t) + j_t([L^\dagger, X])dB(t),$$
(A4)

which is also called the QSDE. The field operator changes to $\tilde{B}(t) = j_t[B(t)]$ and satisfies the output equation

$$d\tilde{B}(t) = j_t(L)dt + dB(t).$$
(A5)

Let us assume that the probe is a coherent field with amplitude α. Then the expectation $\langle X(t)\rangle$ obeys

$$\frac{d\langle X(t)\rangle}{dt} = \left\langle j_t\left(i[H', X] + L^\dagger XL - \tfrac{1}{2}L^\dagger LX - \tfrac{1}{2}XL^\dagger L\right)\right\rangle,$$

where $H' = H + (\alpha L^\dagger - \alpha^* L)/2i$. In the Schrödinger picture the expectation $\langle X(t)\rangle$ is represented in terms of the time-dependent unconditional state $\rho(t)$ as $\langle X(t)\rangle = \text{Tr}[X\rho(t)]$. Then it is easy to find that $\rho(t)$ obeys the master equation (1):

$$\frac{d\rho}{dt} = -i[H, \rho] + \mathcal{D}[L]\rho, \quad \mathcal{D}[L]\rho = L\rho L^\dagger - \tfrac{1}{2}L^\dagger L\rho - \tfrac{1}{2}\rho L^\dagger L,$$
(A6)

where H' has been replaced by H. Note finally that, if the system interacts with m probe fields, then the resulting master equation is given by

$$\frac{d\rho}{dt} = -i[H, \rho] + \sum_{k=1}^m \mathcal{D}[L_k]\rho.$$
(A7)

2. Derivation of the series product formula (2)

The series product formula (2),

$$G_1 \triangleright G_2 = \left(L_1 + L_2, H_1 + H_2 + \frac{1}{2i}(L_2^\dagger L_1 - L_1^\dagger L_2) \right), \quad \text{(A8)}$$

is directly obtained from Eq. (A3) as follows. Because the single probe field represented by $B(t)$ first interacts with the system $G_1 = (L_1, H_1)$ and secondly with $G_2 = (L_2, H_2)$, the change of the total unitary operator $U(t)$ is given by

$$
\begin{aligned}
U&(t + dt) \\
&= \left[I - \left(iH_2 + \frac{1}{2}L_2^\dagger L_2 \right)dt + L_2 dB^\dagger(t) - L_2^\dagger dB(t) \right] \\
&\quad \times \left[I - \left(iH_1 + \frac{1}{2}L_1^\dagger L_1 \right)dt \right. \\
&\qquad \left. + L_1 dB^\dagger(t) - L_1^\dagger dB(t) \right] U(t) \\
&= \left\{ I - i\left[H_1 + H_2 + \frac{1}{2i}(L_2^\dagger L_1 - L_1^\dagger L_2) \right]dt \right. \\
&\qquad - \frac{1}{2}(L_1 + L_2)^\dagger(L_1 + L_2)dt \\
&\qquad \left. + (L_1 + L_2)dB^\dagger(t) - (L_1 + L_2)^\dagger dB(t) \right\} U(t).
\end{aligned}
$$

This means that the whole system $G_1 \triangleright G_2$ is characterized by Eq. (2) or (A8). Note that, if G_1 and G_2 are different systems (for example, G_1 is a qubit and G_2 is an amplifier), then (L_1, H_1) and (L_2, H_2) are operators on the respective Hilbert spaces, and the more precise expression of the operators appearing in Eq. (A8) is, e.g., $L_1 \otimes I + I \otimes L_2$.

3. General SLH formula

A more general Markovian open quantum system, which couples with m independent probe fields $B(t) = [B_1(t), \ldots, B_m(t)]^\top$, is characterized by the triplet (S, L, H), where S is an $m \times m$ unitary matrix representing the scattering process of the probe fields. In this case the QSDE is represented by [23]

$$
\begin{aligned}
dU(t) = \Big\{ &- \left(iH + \tfrac{1}{2}L^\dagger L \right)dt + \mathrm{Tr}[(S - I)d\Lambda(t)^T] \\
&+ dB(t)^\dagger L - L^\dagger S dB(t) \Big\} U(t),
\end{aligned}
$$

with $U(0) = I$, where $L = [L_1, \ldots, L_m]^\top$ is a vector of coupling operators, $\Lambda = (\Lambda_{ij})$ is the matrix of gauge process operators satisfying $d\Lambda_{ij}d\Lambda_{k\ell} = \delta_{jk}d\Lambda_{i\ell}$, and H is a system Hamiltonian. It is shown in [23] that the cascade connection from $G_1 = (S_1, L_1, H_1)$ to $G_2 = (S_2, L_2, H_2)$ is given by

$$
\begin{aligned}
G_1 \triangleright G_2 = \Big(&S_2 S_1, L_2 + S_2 L_1, H_1 + H_2 \\
&+ \frac{1}{2i}(L_2^\dagger S_2 L_1 - L_1^\dagger S_2^\dagger L_2) \Big).
\end{aligned}
$$

The proposed CF-controlled system (3) can then be equivalently represented by

$$G = (1, L_1, H_{\text{sys}}) \triangleright (e^{i\phi}, 0, 0) \triangleright (1, L_2, 0),$$
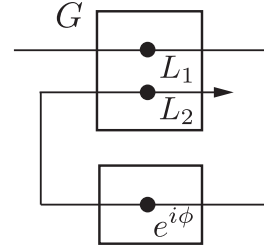

FIG. 7. Coherent feedback configuration for the system G, composed of two couplings L_1 and L_2, and the phase shifter $e^{i\phi}$ placed along the feedback loop.

where $(e^{i\phi}, 0, 0)$ represents a static device that only changes the phase of the field, such as a $\pi/2$ wave plate; that is, a phase shifter is placed along the feedback loop between the two systems, as shown in Fig. 7 below.

APPENDIX B: PROOF OF UNIQUENESS OF $|\Phi_j\rangle$ FOR THE QUTRIT STABILIZATION PROBLEM

Here we prove that, in the ideal setup, one of the vectors $\{|\Phi_1\rangle, |\Phi_2\rangle, |\Phi_3\rangle\}$ given in Sec. IV A can be selectively assigned as the unique pure steady state of the CF-controlled system, by properly choosing the parameters (u_1, u_2) in the added Hamiltonian H_{sys} given by Eq. (8). First let us determine the parameter (u_1, u_2), using Theorem 1 given in Sec. III A; that is, $|\Phi_i\rangle$ is a steady state of the master equation (1) if and only if it is an eigenvector of both L and $iH + L^\dagger L/2$. Now $\{|\Phi_1\rangle, |\Phi_2\rangle, |\Phi_3\rangle\}$ are eigenvectors of L in Eq. (7). Then for $|\Phi_1\rangle$ to be a steady state, it must be an eigenvector of $iH + L^\dagger L/2$:

$$
iH + \frac{1}{2}L^\dagger L = \begin{bmatrix} (\kappa + \gamma)/2 & u_1 & 0 \\ -u_1 & \gamma/2 & u_2 - \sqrt{\kappa\gamma} \\ 0 & -u_2 & \kappa/2 \end{bmatrix}.
$$

That is,

$$
\begin{aligned}
&\begin{bmatrix} (\kappa + \gamma)/2 & u_1 & 0 \\ -u_1 & \gamma/2 & u_2 - \sqrt{\kappa\gamma} \\ 0 & -u_2 & \kappa/2 \end{bmatrix} \begin{bmatrix} 2\kappa \\ 2\sqrt{\kappa\gamma} \\ \gamma \end{bmatrix} \\
&= \begin{bmatrix} \kappa(\kappa + \gamma) + 2u_1\sqrt{\kappa\gamma} \\ -2u_1\kappa + u_2\gamma \\ -2u_2\sqrt{\kappa\gamma} + \kappa\gamma/2 \end{bmatrix} = \lambda \begin{bmatrix} 2\kappa \\ 2\sqrt{\kappa\gamma} \\ \gamma \end{bmatrix}
\end{aligned}
$$

must hold, where λ is an eigenvalue. This immediately yields $(u_1, u_2) = (-\sqrt{\kappa\gamma}/2, 0)$, with $\lambda = \kappa/2$. Similarly we obtain $(u_1, u_2) = (0, \sqrt{\kappa\gamma}/2)$ for the case $|\Phi_2\rangle$ and $u_2 = \sqrt{\kappa\gamma}$ for the case $|\Phi_3\rangle$.

Now, by using the following result, we prove that $|\Phi_i\rangle$ is a *unique* steady state.

Theorem 2 [52]. Let $\mathcal{D}$ be the subset composed of pure steady states (called the "dark states") of the Markovian master equation (A7) in the Hilbert space $\mathcal{H}$. If there is no subspace $\mathcal{S} \subseteq \mathcal{H}$ with $\mathcal{S} \perp \mathcal{D}$ such that $L_k \mathcal{S} \subseteq \mathcal{S}$ for all k, then $\mathcal{D}$ is the unique subset of steady states.

For the case $|\Phi_1\rangle$, $\mathcal{D}$ is given by $\mathcal{D} = \text{span}\{|\Phi_1\rangle\}$. Then it is easy to find that the subspace orthogonal to $\mathcal{D}$ is

$$\mathcal{S} = \text{span}\left\{\begin{bmatrix} \gamma \\ 0 \\ -2\kappa \end{bmatrix}, \begin{bmatrix} 0 \\ \sqrt{\gamma} \\ -2\sqrt{\kappa} \end{bmatrix}\right\}.$$

Then, we have

$$L\mathcal{S} = \text{span}\left\{\begin{bmatrix} \gamma\sqrt{\kappa} \\ \gamma\sqrt{\gamma} \\ 2\kappa\sqrt{\kappa} \end{bmatrix}, \begin{bmatrix} 0 \\ 0 \\ 1 \end{bmatrix}\right\},$$

which clearly shows that $L\mathcal{S} \nsubseteq \mathcal{S}$. Therefore, from Theorem 2, $|\Phi_1\rangle$ is the unique steady state of the master equation of the system (L, H) with $(u_1, u_2) = (-\sqrt{\kappa\gamma}/2, 0)$. Then, from the equivalency of the uniqueness of the steady state and the deterministic convergence to it for a finite-dimensional Markovian quantum system [50], we arrive at the conclusion that any initial state $\rho(0)$ converges to $|\Phi_i\rangle$. Similarly, we can prove the uniqueness of $|\Phi_2\rangle$ and $|\Phi_3\rangle$.

APPENDIX C: LINEAR OPEN QUANTUM SYSTEMS

1. General single-mode linear model

Here we describe the QSDE of a general single-mode open harmonic oscillator that interacts with a single field; for a general system composed of multiple harmonic oscillators, see [4,6]. This system is generally characterized by the quadratic Hamiltonian

$$H = \frac{1}{2}x^\top G x = \frac{1}{2}[q, p]\begin{bmatrix} g_1 & g_2 \\ g_2 & g_3 \end{bmatrix}\begin{bmatrix} q \\ p \end{bmatrix}, \ g_i \in \mathbb{R},$$

and the coupling operator $L = c_1 q + c_2 p$ ($c_1, c_2 \in \mathbb{C}$), where $x = [q, p]^\top$ is the vector of canonical variables of the oscillator, satisfying $qp - pq = i$. Note that, from Eq. (A2), the oscillator couples with the field via the following interaction Hamiltonian:

$$H_{\text{int}}(t + dt, t) = i(c_1 q + c_2 p)dB^\dagger(t) - i(c_1 q + c_2 p)^\dagger dB(t).$$

Then the QSDEs (A4) of $q(t) = j_t(q)$ and $p(t) = j_t(p)$, for the system (L, H) described above, are given by

$$dq(t) = [g_2 + \text{Im}(c_1 c_2^*)]q(t)dt + g_3 p(t)dt$$
$$\qquad - ic_2^* dB(t) + ic_2 dB^\dagger(t),$$
$$dp(t) = -g_1 q(t)dt - [g_2 + \text{Im}(c_1^* c_2)]p(t)dt$$
$$\qquad + ic_1^* dB(t) - ic_1 dB^\dagger(t).$$

This set of equations can be summarized as

$$dx(t) = Ax(t)dt + i\Sigma[C^\top dB^\dagger(t) - C^\dagger dB(t)], \quad \text{(C1)}$$

where $x(t) = [q(t), p(t)]^\top$,

$$A := \Sigma[G + \text{Im}(C^\dagger C)], \ C = [c_1, c_2], \ \Sigma = \begin{bmatrix} 0 & 1 \\ -1 & 0 \end{bmatrix}.$$

Also the output field operator (A5) is expressed as

$$d\tilde{B}(t) = Cx(t)dt + dB(t). \quad \text{(C2)}$$

Due to the linearity of Eq. (C1), the quantum state $\rho(t)$ is Gaussian for all t, if $\rho(0)$ is Gaussian. Then the system is fully characterized by the mean vector $\langle x(t) \rangle = [\langle q(t) \rangle, \langle p(t) \rangle]^\top$ and the covariance matrix

$$V(t) = \begin{bmatrix} \langle \Delta q(t)^2 \rangle & \star \\ \langle \Delta q(t)\Delta p(t) + \Delta p(t)\Delta q(t) \rangle/2 & \langle \Delta p(t)^2 \rangle \end{bmatrix},$$

where $\Delta q = q - \langle q \rangle$ and $\Delta p = p - \langle p \rangle$, and $\star$ denotes the symmetric element. The dynamics of $\langle x(t) \rangle$ is readily obtained as $d\langle x(t) \rangle/dt = A\langle x(t) \rangle$, where the field state is assumed to be the vacuum. Also from the quantum Ito rule (A1), the time evolution equation of $V(t)$ is obtained as

$$\frac{d}{dt}V(t) = AV(t) + V(t)A^\top + D, \quad \text{(C3)}$$

where $D = \Sigma \text{Re}(C^\dagger C)\Sigma^\top$. It is known that, if all the eigenvalues of A have negative real part, the mean vector $\langle x(t) \rangle$ converges to zero and Eq. (C3) has a unique steady solution $V(\infty)$.

2. Steady covariance matrix for the spin squeezing problem

We here apply the above formulas to our model, and derive the dynamical equations of the system variables $(q(t), p(t))$ and the covariance matrix $V(t)$. Now the system is an open quantum harmonic oscillator driven by the following Hamiltonian and the coupling operator:

$$H = -\frac{\sqrt{\kappa\gamma}}{2}(qp + pq), \ L = (\sqrt{\kappa} + \sqrt{\gamma})q + i\sqrt{\gamma}p$$

Hence, by definition we find

$$G = \begin{bmatrix} 0 & -\sqrt{\kappa\gamma} \\ -\sqrt{\kappa\gamma} & 0 \end{bmatrix}, \ C = [\sqrt{\kappa} + \sqrt{\gamma}, i\sqrt{\gamma}].$$

Then A and D in Eqs. (C1) and (C3) are obtained as follows:

$$A = \begin{bmatrix} -2\sqrt{\kappa\gamma} - \gamma & 0 \\ 0 & -\gamma \end{bmatrix}, \ D = \begin{bmatrix} \gamma & 0 \\ 0 & (\sqrt{\kappa} + \sqrt{\gamma})^2 \end{bmatrix}.$$

Hence, the differential equation (C3) has the following unique steady solution:

$$V(\infty) = \frac{1}{2}\begin{bmatrix} \sqrt{\gamma}/(2\sqrt{\kappa} + \sqrt{\gamma}) & 0 \\ 0 & (\sqrt{\kappa} + \sqrt{\gamma})^2/\gamma \end{bmatrix}.$$

[1] A. Furusawa and P. van Loock, *Quantum Teleportation and Entanglement: A Hybrid Approach to Optical Quantum Information Processing* (Wiley-VCH, Berlin, 2011).

[2] V. P. Belavkin, On the theory of controlling observable quantum systems, Autom. Remote Control **44**, 178 (1983).

[3] L. Bouten, R. van Handel, and M. R. James, A discrete invitation to quantum filtering and feedback control, SIAM Rev. **51**, 239 (2009).

[4] H. M. Wiseman and G. J. Milburn, *Quantum Measurement and Control* (Cambridge University, Cambridge, England, 2009).

[5] K. Jacobs, *Quantum Measurement Theory and its Applications* (Cambridge University, Cambridge, England, 2014).

[6] H. I. Nurdin and N. Yamamoto, *Linear Dynamical Quantum Systems: Analysis, Synthesis, and Control* (Springer, New York, 2017).

[7] L. Thomsen, S. Mancini, and H. M. Wiseman, Continuous quantum nondemolition feedback and unconditional atomic spin squeezing, J. Phys. B **35**, 4937 (2002).

[8] R. van Handel, J. K. Stockton, and H. Mabuchi, Feedback control of quantum state reduction, IEEE Trans. Automat. Contr. **50**, 768 (2005).

[9] J. M. Geremia, Deterministic and Nondestructively Verifiable Preparation of Photon Number States, Phys. Rev. Lett. **97**, 073601 (2006).

[10] M. Yanagisawa, Quantum Feedback Control for Deterministic Entangled Photon Generation, Phys. Rev. Lett. **97**, 190201 (2006).

[11] A. Negretti, U. V. Poulsen, and K. Molmer, Quantum Superposition State Production by Continuous Observations and Feedback, Phys. Rev. Lett. **99**, 223601 (2007).

[12] N. Yamamoto, K. Tsumura, and S. Hara, Feedback control of quantum entanglement in a two-spin system, Automatica **43**, 981 (2007).

[13] M. Mirrahimi and R. van Handel, Stabilizing feedback controls for quantum systems, SIAM J. Control Optim. **46**, 445 (2007).

[14] C. Sayrin, I. Dotsenko, X. Zhou, B. Peaudecerf, T. Rybarczyk, S. Gleyzes, P. Rouchon, M. Mirrahimi, H. Amini, M. Brune, J.-M. Raimond, and S. Haroche, Real-time quantum feedback prepares and stabilizes photon number states, Nature **477**, 73 (2011).

[15] R. Vijay *et al.*, Stabilizing Rabi oscillations in a superconducting qubit using quantum feedback, Nature (London) **490**, 77 (2012).

[16] P. Campagne-Ibarcq, E. Flurin, N. Roch, D. Darson, P. Morfin, M. Mirrahimi, M. H. Devoret, F. Mallet, and B. Huard, Persistent Control of a Superconducting Qubit by Stroboscopic Measurement Feedback, Phys. Rev. X **3**, 021008 (2013).

[17] D. Riste *et al.*, Deterministic entanglement of superconducting qubits by parity measurement and feedback, Nature (London) **502**, 350 (2013).

[18] R. Inoue, S. Tanaka, R. Namiki, T. Sagawa, and Y. Takahashi, Unconditional Quantum-Noise Suppression Via Measurement-Based Quantum Feedback, Phys. Rev. Lett. **110**, 163602 (2013).

[19] K. C. Cox, G. P. Greve, J. M. Weiner, and J. K. Thompson, Deterministic Squeezed States with Collective Measurements and Feedback, Phys. Rev. Lett. **116**, 093602 (2016).

[20] H. M. Wiseman and G. J. Milburn, All-optical versus electro-optical quantum-limited feedback, Phys. Rev. A **49**, 4110 (1994).

[21] M. Yanagisawa and H. Kimura, Transfer function approach to quantum control—part I: Dynamics of quantum feedback systems, IEEE Trans. Autom. Control **48**, 2107 (2003).

[22] M. R. James, H. I. Nurdin, and I. R. Petersen, H_∞ control of linear quantum stochastic systems, IEEE Trans. Automat. Contr. **53**, 1787 (2008).

[23] J. Gough and M. R. James, The series product and its application to quantum feedforward and feedback networks, IEEE Trans. Automat. Cont. **54**, 2530 (2009).

[24] H. I. Nurdin, M. R. James, and I. R. Petersen, Coherent quantum LQG control, Automatica **45**, 1837 (2009).

[25] R. Hamerly and H. Mabuchi, Advantages of Coherent Feedback for Cooling Quantum Oscillators, Phys. Rev. Lett. **109**, 173602 (2012).

[26] N. Yamamoto, Coherent Versus Measurement Feedback: Linear Systems Theory for Quantum Information, Phys. Rev. X **4**, 041029 (2014).

[27] A. L. Grimsmo, Time-Delayed Quantum Feedback Control, Phys. Rev. Lett. **115**, 060402 (2015).

[28] A. Balouchi and K. Jacobs, Coherent versus measurement-based feedback for controlling a single qubit, Quantum Sci. Technol. **2**, 025001 (2017).

[29] H. Mabuchi, Coherent-feedback quantum control with a dynamic compensator, Phys. Rev. A **78**, 032323 (2008).

[30] S. Iida, M. Yukawa, H. Yonezawa, N. Yamamoto, and A. Furusawa, Experimental demonstration of coherent feedback control on optical field squeezing, IEEE Trans. Automat. Contr. **57**, 2045 (2012).

[31] S. Shankar *et al.*, Autonomously stabilized entanglement between two superconducting quantum bits, Nature (London) **504**, 419 (2013).

[32] J. Kerckhoff, R. W. Andrews, H. S. Ku, W. F. Kindel, K. Cicak, R. W. Simmonds, and K. W. Lehnert, Tunable Coupling to a Mechanical Oscillator Circuit Using a Coherent Feedback Network, Phys. Rev. X **3**, 021013 (2013).

[33] Y. Liu, S. Shankar, N. Ofek, M. Hatridge, A. Narla, K. M. Sliwa, L. Frunzio, R. J. Schoelkopf, and M. H. Devoret, Comparing and Combining Measurement-Based and Driven-Dissipative Entanglement Stabilization, Phys. Rev. X **6**, 011022 (2016).

[34] M. Sarovar *et al.*, Silicon nanophotonics for scalable quantum coherent feedback networks, EPJ Quantum Technology **3**, 14 (2016).

[35] K. Hammerer, K. Molmer, E. S. Polzik, and J. I. Cirac, Light-matter quantum interface, Phys. Rev. A **70**, 044304 (2004).

[36] M. Takeuchi, S. Ichihara, T. Takano, M. Kumakura, T. Yabuzaki, and Y. Takahashi, Spin Squeezing Via One-Axis Twisting with Coherent Light, Phys. Rev. Lett. **94**, 023003 (2005).

[37] J. F. Sherson and K. Molmer, Polarization Squeezing by Optical Faraday Rotation, Phys. Rev. Lett. **97**, 143602 (2006).

[38] I. D. Leroux, M. H. Schleier-Smith, and V. Vuletic, Implementation of Cavity Squeezing of a Collective Atomic Spin, Phys. Rev. Lett. **104**, 073602 (2010).

[39] M. H. Schleier-Smith, I. D. Leroux, and V. Vuletic, Squeezing the collective spin of a dilute atomic ensemble by cavity feedback, Phys. Rev. A **81**, 021804(R) (2010).

[40] K. W. Murch, U. Vool, D. Zhou, S. J. Weber, S. M. Girvin, and I. Siddiqi, Cavity-Assisted Quantum Bath Engineering, Phys. Rev. Lett. **109**, 183602 (2012).

[41] E. G. Dalla Torre, J. Otterbach, E. Demler, V. Vuletic, and M. D. Lukin, Dissipative Preparation of Spin Squeezed Atomic Ensembles in a Steady State, Phys. Rev. Lett. **110**, 120402 (2013).

[42] M. Wang, W. Qu, P. Li, H. Bao, V. Vuletic, and Y. Xiao, Two-axis-twisting spin squeezing by multipass quantum erasure, Phys. Rev. A **96**, 013823 (2017).

[43] H. J. Carmichael, Quantum Trajectory Theory for Cascaded Open Systems, Phys. Rev. Lett. **70**, 2273 (1993).

[44] C. W. Gardiner and P. Zoller, *Quantum Noise* (Springer, Berlin, 2004).

[45] J. Gambetta, A. Blais, M. Boissonneault, A. A. Houck, D. I. Schuster, and S. M. Girvin, Quantum trajectory approach to circuit QED: Quantum jumps and the Zeno effect, Phys. Rev. A **77**, 012112 (2008).

[46] K. W. Murch, S. J. Weber, C. Macklin, and I. Siddiqi, Observing single quantum trajectories of a superconducting quantum bit, Nature (London) **502**, 211 (2013).

[47] S. J. Weber *et al.*, Mapping the optimal route between two quantum states, Nature (London) **511**, 570573 (2014).

[48] S. Hacohen-Gourgy *et al.*, Quantum dynamics of simultaneously measured non-commuting observables, Nature (London) **538**, 491 (2016).

[49] S. Hacohen-Gourgy, L. P. Garcia-Pintos, L. S. Martin, J. Dressel, and I. Siddiqi, Incoherent Qubit Control Using the Quantum Zeno Effect, Phys. Rev. Lett. **120**, 020505 (2018).

[50] S. G. Schirmer and X. Wang, Stabilizing open quantum systems by Markovian reservoir engineering, Phys. Rev. A **81**, 062306 (2010).

[51] N. Yamamoto, Parametrization of the feedback Hamiltonian realizing a pure steady state, Phys. Rev. A **72**, 024104 (2005).

[52] B. Kraus *et al.*, Preparation of entangled states by quantum Markov processes, Phys. Rev. A **78**, 042307 (2008).

[53] R. Bianchetti, S. Filipp, M. Baur, J. M. Fink, C. Lang, L. Steffen, M. Boissonneault, A. Blais, and A. Wallraff, Control and Tomography of a Three Level Superconducting Artificial Atom, Phys. Rev. Lett. **105**, 223601 (2010).

[54] O. Kyriienko and A. S. Sorensen, Continuous-Wave Single-Photon Transistor Based on a Superconducting Circuit, Phys. Rev. Lett. **117**, 140503 (2016).

[55] T. Holstein and H. Primakoff, Field dependence of the intrinsic domain magnetization of a ferromagnet, Phys. Rev. **58**, 1098 (1940).

[56] L. Ma, X. Wang, C. Sun, and F. Nori, Quantum spin squeezing, Phys. Rep. **509**, 89 (2011).

[57] J. Kerckhoff, H. I. Nurdin, D. S. Pavlichin, and H. Mabuchi, Designing Quantum Memories with Embedded Control: Photonic Circuits for Autonomous Quantum Error Correction, Phys. Rev. Lett. **105**, 040502 (2010).

[58] K. Fujii, M. Negoro, N. Imoto, and M. Kitagawa, Measurement-free Topological Protection Using Dissipative Feedback, Phys. Rev. X **4**, 041039 (2014).

[59] M. R. James and J. Gough, Quantum dissipative systems and feedback control design by interconnection, IEEE Trans. Automat. Cont. **55**, 1806 (2010).